Endothelial Fenestral Diaphragms: A Quick-Freeze, Deep-Etch Study

ELAINE L. BEARER and LELIO ORCI *with the technical assistance of* PATRICK SORS
Institute of Histology and Embryology, University of Geneva, Switzerland. Dr. Bearer's present address is Department of Pathology, University of California, San Francisco, California 94143.

ABSTRACT The route by which water, solutes, and macromolecules traverse the endothelial cell has long been a subject of study for both physiologists and cell biologists. Recent physiologic studies describe a slit-shaped pore (5.1–5.7-nm wide) as the communicating channel, although no channel of such dimensions has been visible in electron microscopic preparations. That this channel should be found within the fenestral diaphragm has long been suggested. In this report, by the aid of a new technique in tissue processing, we are able to demonstrate a possible morphologic correlate within the fenestral diaphragm of fenestrated capillaries. Quick-freezing and deep-etching of whole tissue blocks allows the sublimation of water from the endothelial pores, thus leaving the channels through the diaphragms empty and readily replicated with a platinum–carbon shadow. The structure of the diaphragm was revealed thus to be composed of radial fibrils of 7 nm in diameter, interweaving in a central mesh, and creating by their geometric distribution, wedge-shaped channels around the periphery of the pore. The average channel had a maximum arc length of 5.46 nm. Fenestrated endothelia from various tissues, including endocrine and exocrine pancreas, adrenal cortex, and kidney peritubular capillaries, displayed the same diaphragmatic structure, whereas continuous capillaries in muscle had no such diaphragm. Photographic augmentation of electron micrographs of etched replicas displayed marked enhancement at $n = 8$, confirming an octagonal symmetry of the fenestral diaphragm. Finally, cationic ferritin, clearly visible as a marker after etching, heavily bound to the flowerlike structure within the fenestral pore. We conclude that the fenestral diaphragm contains the structure responsible for fenestrated capillary permeability and that the communicating channel has the shape of a wedge.

Blood-borne substances must pass through the endothelial cell to gain access to tissue compartments, and conversely, tissue substances traverse the endothelial cells to enter the circulation. Yet little is known about the channels through which both water and selected solutes must pass. Indirect evidence of the size, shape, and properties of the channels has been gleaned from those physiologic and morphologic studies that have produced somewhat conflicting information: the former, focusing on the continuous nonfenestrated capillary of muscle, very early defined two pore sizes, a prevalent size of 6 nm and a rare pore of 50–70 nm in diameter (1–5). Traditional electron microscopic examination of somatic capillaries do reveal plasmalemmal vesicles with 50-nm openings, but these occur too frequently to be the physiologic "rare" pore. Extrapolation of these physiologic parameters to the fenestral capillaries of many visceral tissues is equally unproductive inasmuch as electron microscopy of these disclosed only large (60–70-nm diam) porelike depressions in freeze-fracture replicas, which again, are too large to be the prevalent and too frequent to be the rare pore (6). Across the pore of all but glomerular fenestrations and some plasmalemmal vesicles is a diaphragm (7). These diaphragms have been hypothesized to be modifications of the same structure (8). Tracer studies, in which electron-dense molecules of various sizes and charges are perfused and allowed to gain access to tissue, have demonstrated differences between them. Horseradish peroxidase (4.5-nm diam) passes freely through both diaphragms. Ferritin, which is larger (11-nm diam), passes through only a small percentage of fenestrated diaphragms, showing that the diaphragm must perform a filtration function (8, 9). Selective passage of such tracers correlates well with physiologic measurements of the permeability of mole-

THE JOURNAL OF CELL BIOLOGY · VOLUME 100 FEBRUARY 1985 418–428

cules of differing sizes through the continuous capillary wall. This correlation, coupled with the observation of clouds of tracer on the abluminal side of fenestral diaphragms and inside plasmalemmal vesicles, leads to the assumption that the true communicating channels are within the diaphragms that bridge the morphologic pores (8).

In an elegant attempt to describe the structure of the fenestral diaphragm, Gert Maul (10) did photographic augmentation of micrographs of both grazing sections and freeze-fractures of fenestrated endothelial pores, and showed that they might be composed of two concentric rings connected by fibrils, perhaps arranged in an octagonal symmetry. He also found that the size and postulated internal structure were polymorphic, in that only 8 of 20 micrographs could be photographically superimposed. More recently, the composition of the diaphragm has been investigated by Simionescu et al. (11), who have shown that only heparinase can abolish the binding of cationic ferritin (CF)[1] to the fenestral diaphragm. Furthermore, differences between the diaphragm of the plasmalemmal vesicle and the fenestrae are becoming apparent through these studies. Although initially the two diaphragms appeared similar, both being unilaminar and each having a central density, it has now been shown that the fenestral diaphragm binds no lectins at pH 7.4 (12), reacts within seconds with CF (13), and loses this reactivity after heparinase treatment (11). Conversely, the plasmalemmal diaphragm binds lectins (12), is not reactive to CF (13), and appears unperturbed by heparinase (11). Previous tracer studies also differentiate between the two and confirm physiologic evidence (1) that shows continuous capillaries to be more permeable to large molecules than fenestrated capillaries.

In this study we show the internal structure of the fenestral and plasmalemmal diaphragms, and the true communicating channels within them. We show that these two types of diaphragm are dissimilar to each other, but that each structure displays similar configurations in different tissues, such as muscle, endocrine and exocrine glands, and kidney. To do this we have used a simple method of quick-freezing and deep-etching of whole tissues. We furthermore compare these diaphragms with those seen in tissue prepared by traditional methods. Finally, we calculate the dimensions of the communicating channel and compare this with the dimensions obtained from previous physiologic and tracer studies.

MATERIALS AND METHODS

Tissue Preparation: SiVZ rats, at 6–8 wk after birth and weighing not <250 g, were anesthetized by intraperitoneal injection of nembutal (0.2 ml/100 g). Perfusion through the left ventricle of the heart, at a pressure of 80–100 mmHg, was begun for 3–5 min with phosphate-buffered saline (PBS), warmed to 37°C at pH 7.4, and sometimes containing 2% BSA (Sigma Chemical Co., St. Louis, MO). When renal vessels turned crystal clear, the perfusate was changed to 1.5% glutaraldehyde in 0.1 M sodium cacodylate, 1% sucrose, pH 7.4 (fixative 1), 37°C. Fixation perfusion was allowed to continue for 10 min using ~200 ml of perfusate per animal. Organs were subsequently removed, cut into 1-mm pieces, and incubated for 2 h in the same fixative at room temperature. Fixative containing 0.5% alcian blue was perfused after the same initial steps. Immersion fixation in the same fixative was performed on freshly excised kidney within 3 min of decapitation. CF was injected into the saphenous vein according to Kanwar and Farquhar (14) and allowed to circulate for 25 min before the animal was anesthetized and perfused by the left ventricle, according to the above sequence, except that Karnovsky's fixative replaced fixative 1. Glomeruli were isolated according to Krakower and Greenspan (15) and fixed as above. They were subsequently pelleted and treated as tissue blocks for quick freezing.

[1] *Abbreviation used in this paper:* CF, cationic ferritin.

Quick Freezing: More than 500 individual samples were fixed, frozen, fractured, etched, and observed in the electron microscope.

Fixed tissue, cut into 1-mm blocks and incubated for 20 min in either PBS or distilled water containing 20% methanol, was then mounted on gold specimen holders in the shape of two 1-mm-thick disks 3-mm diam held together by a slightly narrower waist. The specimen holders were stuck onto the epoxy head of a hammer by double-stick tape, and frozen on a liquid nitrogen-cooled copper block by pressing the hammer tightly onto the block for 10 s. The block was made from a copper tube 4-cm diam, 6.2 cm long, 99.99% pure copper, perforated by four holes 1-cm diam symmetrically around the shaft and entering the block 1.7 cm from the top. The center of the shaft was gouged out to within 2 cm of the top face of the block, so that only a 0.5-cm-thick shell remained in the lower end of the cylinder. After all holes had been drilled, the block weighed 410 g. The face of the block was polished like a mirror. The block was put into a styrofoam box and covered with a heavy lead lid which covered the entire face. The box was then filled with liquid nitrogen. When the nitrogen suddenly fizzed up, the block was ready to use. After each time that tissue was frozen against the block, the face was cleaned with cotton soaked in acetone.

The samples were immediately transferred to liquid nitrogen after contact with the block, mounted in a Balzers freeze-fracture device (Balzers, Hudson, NH), and fractured at a gauge temperature of −130°C. The Balzers specimen stage was then allowed to warm to −80°C according to the gauge, and etched in a 10^{-7} Torr vacuum for 20 min. We found that the specimen stage temperature gauge was highly inaccurate, in that at −130°C frozen methanol (melting point −130°C) mounted on a gold holder evaporated within seconds, leaving a shell of frost behind. At −80°C, acetone (melting point −95°C), however, remained solidly frozen, and did not become liquid until −65°C by the gauge. The etching temperature was chosen empirically as being the coldest that we could use and not have recondensation of water in the form of frost on the sample surface. The coldest possible etching temperature was selected to prevent the collapse of fibrils that might occur during a more rapid ice sublimation, as well as to avoid water crystal rearrangements. Etching was followed by rotary platinum shadowing at a 23° angle and six rotations per second, and then by carbon evaporation. Replicas were cleaned immediately in household bleach, followed by a water rinse, then a brief wash in methanol/chloroform (2:1), rinsed in water again, and mounted on carbon- and parlodion-coated Pelco grids. Samples were viewed in a Philips 300 electron microscope (Philips Electronic Instruments, Inc., Mahwah, NJ). All photographs of replicas shown here were photographically reversed.

Glycerol-treated replicas, whether in water or in PBS, were treated the same as the noncryoprotected tissue: that is, they were also etched and replicated on a rotating stage with a low-angle platinum electrode. Quick freezing onto a helium-cooled copper block was performed as described before (16). The tissue was etched and replicated as above.

Freeze Substitution: Tissue was frozen as above on the nitrogen-cooled copper block, then immediately transferred to scintillation counter jars containing 5% OsO_4 in acetone immersed in liquid nitrogen. The tissue was placed face-down onto the frozen acetone. The jars were transferred to a styrofoam box containing dry ice in ethanol and left for 48 h. Then, still at −78°C, the jars were sequentially transferred to −20°X, −4°C, and room temperature for 1 h each. At room temperature, 1% uranyl acetate in 100% ethanol was substituted for the OsO_4 solution. They were finally dehydrated in propylene oxide and embedded in Epon 812. Sections were poststained with aqueous uranyl acetate and lead citrate.

Thin Sections: Fixed tissue was *en bloc* stained with 1% Palade's OsO_4 for 1 h at 4°C, followed by 1% uranyl acetate in Kellenberger's buffer for 1 h at 37°C, dehydrated, and embedded. Grey sections were poststained with uranyl acetate and lead citrate.

Photographic Augmentation: Reversed photographs of etched replicas of endothelia displaying fenestrae were mounted in a Durst enlarger set up at magnifications of 4–5. The photographic paper was rotated around a protractor using the points of the paper as guides for 45° at each turn and exposed thus eight times according to a modification of the method described by Markham et al. (17). The paper was then developed and fixed.

RESULTS

Whole tissue, frozen without glycerol cryoprotection on a simple copper block cooled with liquid nitrogen, was fractured and deeply etched to uncover membrane surfaces, extracellular matrices, and cell coat. After deep etching and rotary shadowing, fenestrated endothelia revealed diaphragms within the 600-Å fenestral pore. The diaphragm was composed of fibrils organized in a flowerlike pattern (Fig. 1, *A–C*). Al-

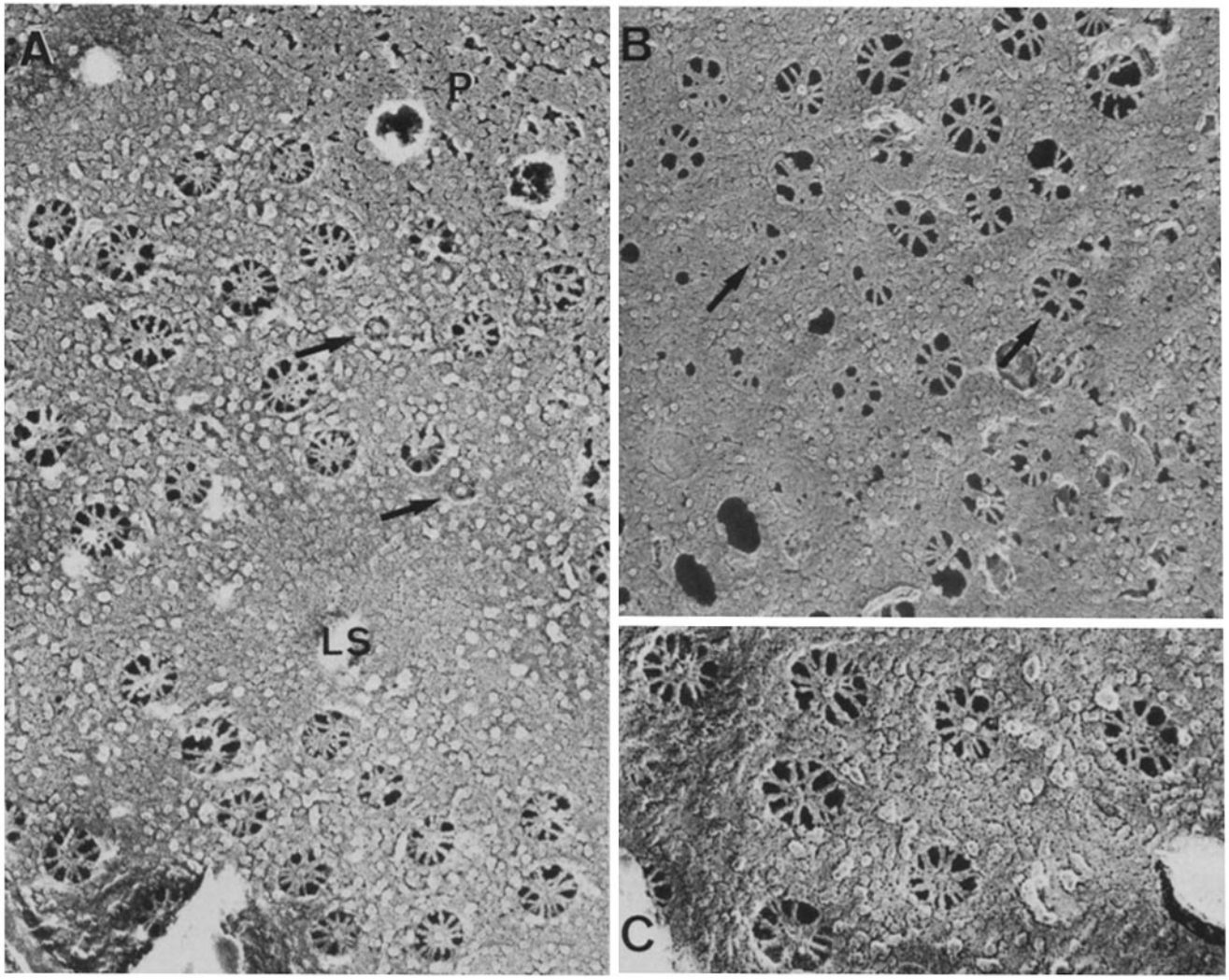

FIGURE 1 (*A*) Fields of fenestral diaphragms on the etched luminal surface (*LS*) of a peritubular capillary in the rat kidney cortex. Holes in the P-fracture face (*P*) correspond to fenestrae that have lost the diaphragm during fracturing. Smaller pores occur among the diaphragms (arrows). × 63,000. (*B*) This P-fracture face displays diaphragms with a rim stolen from the extracellular membrane leaflet (arrow) and the same structure as those seen in surface views. Only a few have a central particle. Holes in the lower left corner correspond to diaphragms torn out during fracturing. (*C*) Slightly higher magnification resolves the many intertwining fibrils that arise from the pore's brim and converge in a central mesh in this luminal surface view. × 120,000.

though the majority of pores contained similar structures, even at low magnification, heterogeneity in the diameter of the pore and in the arrangement of the radiating fibers was apparent. Fenestral diaphragms exhibited the same radial spokes and central mesh when either luminal or abluminal surface was presented to view. In regions where the membrane was cleaved by the fracturing process, they clung to one or the other fracture face, more often to the extracellular (E-face) than to the protoplasmic (P-face), and thus sometimes left holes in either fracture face (Fig. 1 *B*). Those diaphragms remaining in the P-face were encircled by a distinct rim, presumably stolen from the E-face membrane. Fibrils 7-mm wide arising from the pore's brim traversed the opening, weaving a meshwork in the center where they converged (Fig. 1 *C*). The number of fibrils in a given pore ranged from 9 to 21, although fibrils were frequently clustered two and three together, making them difficult to count. In addition, unattached strands, presumably from broken fibrils, occasionally occurred. The central mesh was only sometimes decorated by a small (7–9 nm) particle. This arrangement of fibrils created two types of presumptive communicating channels across the diaphragm for the passage of water and solutes. The first, larger and wedge-shaped, occurred around the periphery of the pore; the second, tiny and square, existed between the densely woven fibrils at the pore's center. In addition to these large fenestral diaphragms, another less common and much smaller opening could be seen on the endothelial cell surface (Fig. 1 *A*). This second type of "pore" was invariably occupied by a large central particle. It was found not only at the periphery of a group of fenestral diaphragms, but it also appeared among them.

In sharp contract to fenestral diaphragms, openings of plasmalemmal vesicles in continuous capillaries of rat diaphragm muscle had no such structure, but instead had much smaller (400 Å) diameter openings. These openings could also be seen in mixed capillaries (those with both vesicles and fenestrae) of the exocrine pancreas and continuous capillaries in kidney medulla. Frequently empty in muscle capillaries,

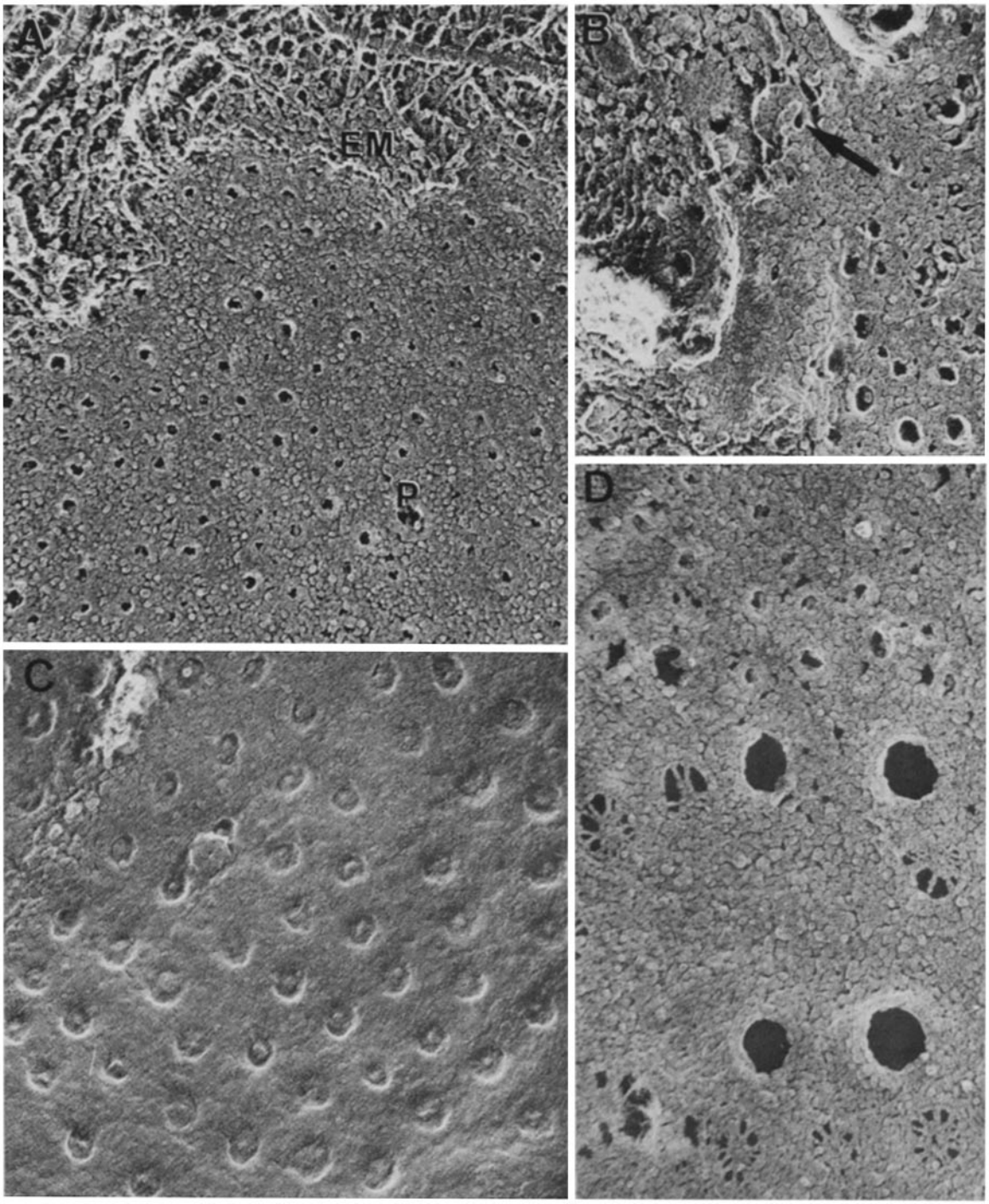

FIGURE 2 (*A*) Plasmalemmal vesicular openings in the P-face (*P*) of a diaphragm muscle capillary. The abluminal surface is recognizable by dense extracellular matrix (*EM*), which obscures the true cell surface. × 60,000. (*B*) A cross-fracture of an endothelial cell in the diaphragm muscle displays a vesicle connected to its opening on the P-face (arrow). × 150,000. (*C*) Lightly etched luminal surface from a continuous capillary in the kidney medulla displays small depressions containing a central particle similar to surface views of muscle capillaries. × 80,000. (*D*) A single capillary in the exocrine pancreas displays both PV openings and fenestral diaphragms side by side in the P-face. × 105,000.

this opening was surrounded by a 10-nm-wide particulate ridge in the abluminal P-face (Fig. 2*A*). These openings were not visible on the abluminal surface. In fortuitous fractures, a vesicle could be seen confluent with the opening in the P-face (Fig. 2*B*). In kidney medulla, luminal surface views of continuous capillaries showed depressions the same size as the holes in the P-face, all of them topped by a large (8.5–10 nm) central particle (Fig. 2*C*). Occasionally in exocrine pancreas, fields of these openings could be seen in the same capillary adjacent to fields of fenestral pores with their unmistakable diaphragm (Fig. 2*D*). Resolution of the structure supporting this central particle was not achieved. The space between the particle and the rim of the opening was too narrow (b = 10 nm) and the below-the-surface depth must

FIGURE 3 (*A*) Deep etching of isolated glomeruli reveals interdigitating pedicels separated from the glomerular capillary by the thick, fibrous basement membrane. The lack of diaphragms across the glomerular capillary fenestrae is in striking contrast to those gracing the peritubular fenestrae (*B*). (*A*) × 75,000; (*B*) × 83,000.

have been too great (a must be <4.4 nm) to allow shadowing at a 23° angle ($\theta = 23°$, $b = 10$ nm, $a = 4.4$ nm) to penetrate.[2] The supporting structure must be, therefore, greater than 4.4 nm below the endothelial cell surface. Lacking diaphragms completely, the fenestrae of glomerular capillaries were empty after etching when viewed from the tissue front, and filled with distant shadows of the lamina rara interna when viewed from the blood front (Fig. 3*A*). The emptiness of these pores was in striking contrast to the diaphragms bridging fenestrae in peritubular capillaries (Fig. 3*B*).

Although the fenestral diaphragms had a consistent basic structure regardless of which surface or fracture face they occupied, or in which tissue they resided, the arrangement of fibrils was as different one from the other as snowflakes. This difference was intensified when tissue was washed and frozen in distilled water, and diminished when postfixed in alcian blue. In tissue frozen in 0.1 M PBS, 87% of fenestral pores had a diameter between 500–700 Å, which equated well with that of glycerinated, buffered freeze-fractures: 500–700 Å (98% of pores) (see Table I). However, in the absence of salts, the pore diameter increased to >700 Å (79% of the pores) (Table I and Fig. 4, *A–C*). This increase in pore diameter was apparent in both traditional glycerol-cryoprotected, no-netched samples when distilled water replaced the standard buffer (Fig. 4*A*), and in freeze-etched samples (Fig. 4*B*). We treated the tissue with alcian blue in an attempt to preserve the diaphragms in the most homogeneous state. Alcian blue is a cationic dye that binds glycosaminoglycans (18), possible

[2] Trigonometric calculation, where b is the base of a right triangle, and a the height, $a = b\tan$, where θ is the angle of the platinum shadow, assuming the replicate to be flat, i.e., parallel to the stage.

TABLE I

Average Pore Diameter

	Diameter				
	<500 Å	500–700 Å	700–930 Å	930 Å	Total counted
	%				(*n*)
Kidney etched					
Frozen in PBS	42	45	13	0	(299)
Frozen in water	2	20	51	26	(112)
Exocrine pancreas etched					
Frozen in water	2	39	45	34	(89)
Kidney cryoprotected					
Glycerol + buffer	15	83	2	0	(321)
Kidney cryoprotected					
Glycerol + water	2	20	41	38	(197)
Kidney, alcian blue etched					
Frozen in water	11	51	32	6	(88)
Total counted					1,195

Micrographs of endothelial from at least five different capillaries in each tissue, and displaying large fields of pores were chosen. All the pores in each micrograph that had a clear brim all the way around the circumference were measured and counted. Measuring was done thus: photocopies were made of each micrograph and the brim of each pore was outlined in pencil. A transparent plastic sheet on which were drawn concentric circles of different diameters was then layered over the photocopy. The pore was classified as having the diameter of the largest circle within which it could fit.

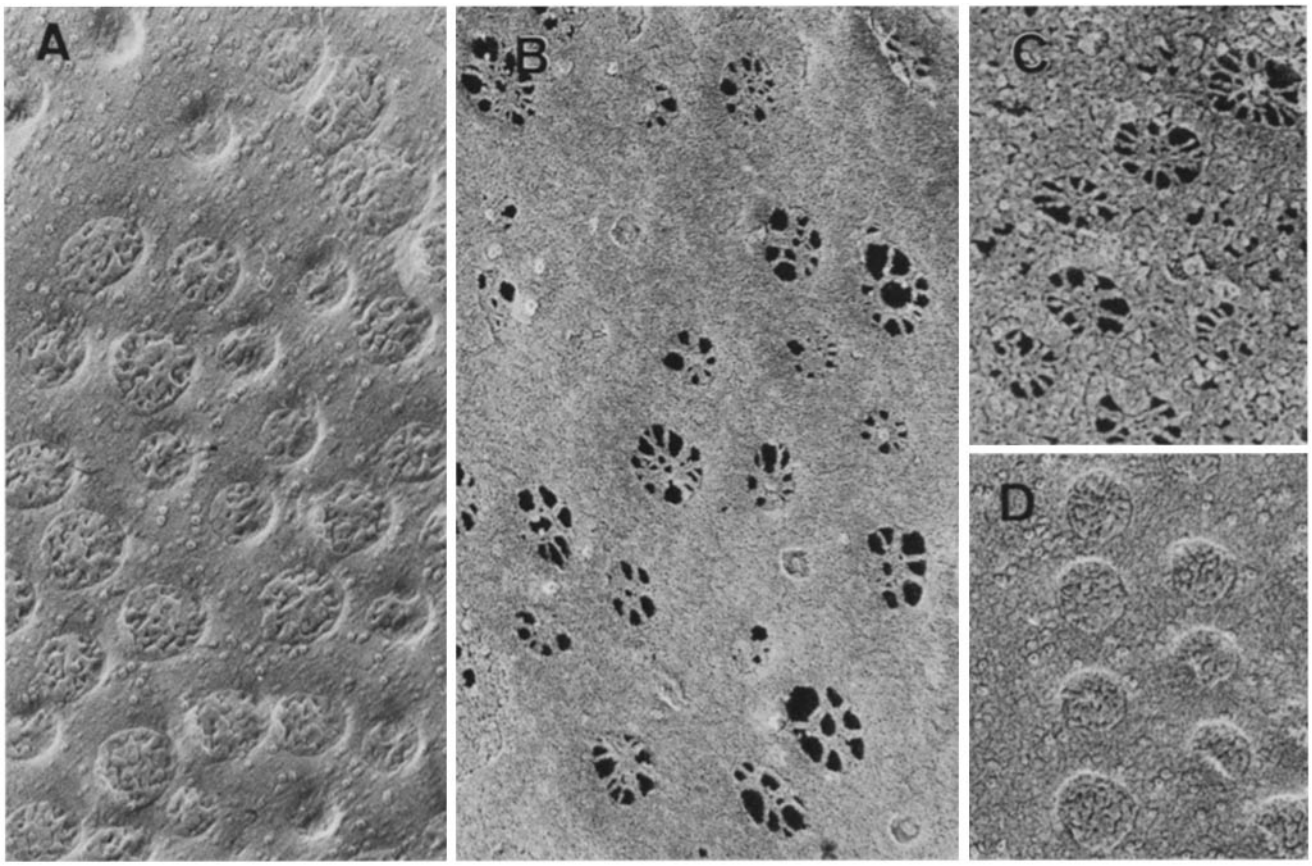

FIGURE 4 (*A*) Kidney cortex, cryoprotected with glycerol in distilled water, shows no diaphragms after 20-min etching, but does disclose a wide variation in fenestral pore size. × 95,000. (*B*) Kidney cortex, quick-frozen without cryoprotection in distilled water, does reveal diaphragms after etching, but also displays wide variation in pore size as well as diaphragmatic structure. × 100,000. (*C*) Alcian-blue perfusion preserves diaphragmatic structure when tissue is quick-frozen in distilled water. × 140,000. (*D*) Alcian blue also preserves pore diameter when kidney is cryoprotected with glycerol and frozen in distilled water. × 100,000.

components of the radial filaments (11). Indeed, alcian blue protected the pore against the effects of distilled water (Table I and Fig. 4, *C* and *D*), since alcian blue-treated endothelia, frozen in distilled water, displayed fenestral diaphragmatic sizes intermediate between those in untreated tissue frozen in physiologic salt and those frozen in water. Despite the alcian blue fixation, polymorphism in diaphragmatic filament arrangement remained, although it was reduced. Immersion

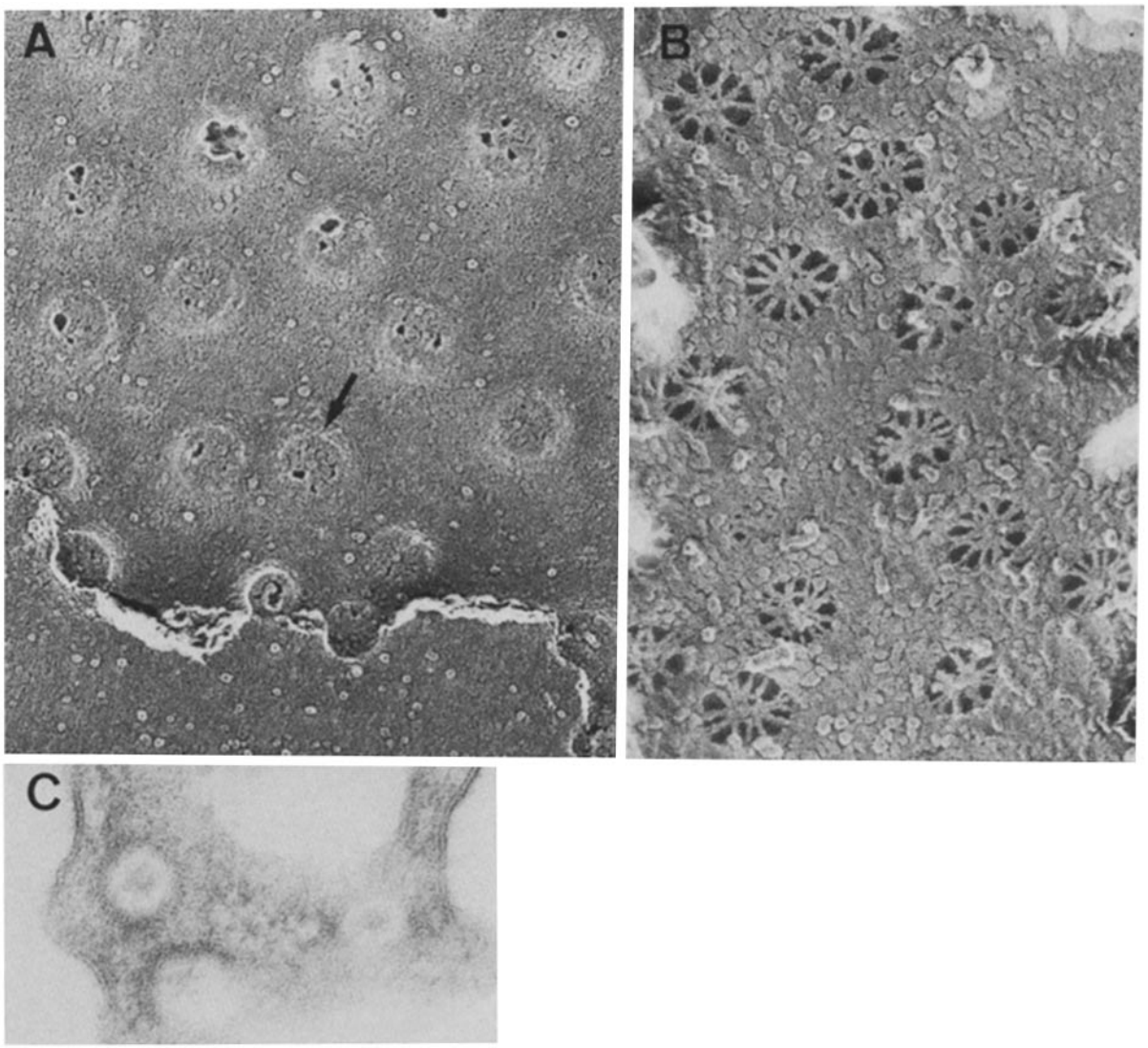

FIGURE 5 (*A*) The E-fracture face of a glycerinated fenestrated peritubular capillary displays little information on diaphragm structure even after 20-min etching and rotary shadowing. The central particle and a hint of radial fibers can be faintly discerned in rare pores (arrow). × 165,000. (*B*) Quick frozen in PBS with 20% methanol and no glycerol, followed by 20-min etching displays internal structure more clearly, but also reveals greater heterogeneity on this luminal surface view. × 130,000. (*C*) Grazing sections disclose faint streaks that radiate from the central density in fenestrae of the same tissue. × 160,000.

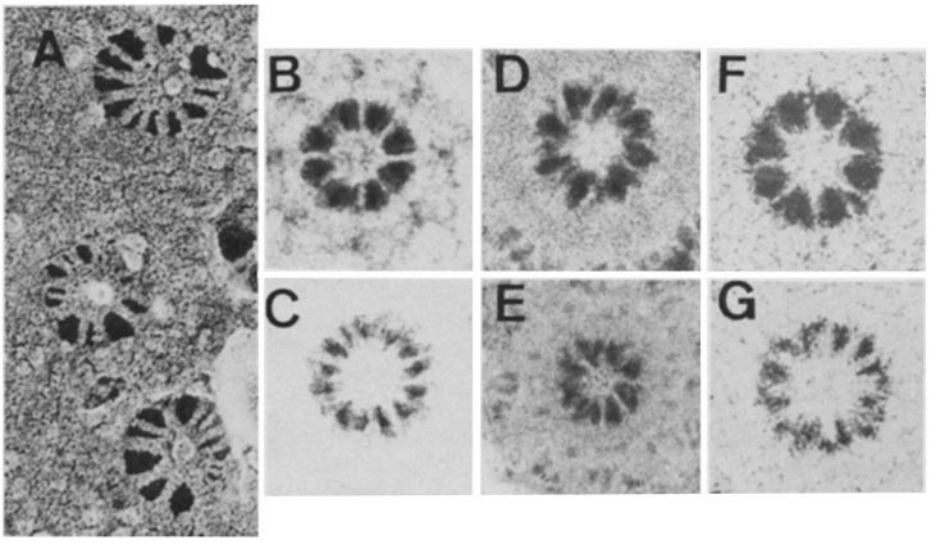

FIGURE 6 (*A*) Capillaries of adrenal cortex display identical fenestral diaphragms as those in kidney cortex. × 215,000. (*B–G*) Photographic augmentation of micrographs from adrenal cortex (*B* + *C*), endocrine pancreas (*D*), exocrine pancreas (*E*), and kidney peritubular capillaries (*F* and *G*) disclose octagonal symmetry when the image was rotated eight times. This symmetry is not readily apparent in the original of the surrenal (*A*) (shown here) at the same magnification as the augmentation (× 215,000). Several fenestrae displayed symmetry of other multiples of 4: 12 (*G*) and 16 (*C*).

fixation had no effect on the basic pore structure, nor did the presence of 2% albumin in the preperfusion wash. Tissue frozen without methanol pretreatment displayed the same diaphragmatic structures, but was less easily etched and had more frequent ice-crystal damage.

As has been previously described (10), glycerinated tissue, etched for 1–2 min, revealed a very faintly discernible structure in fenestral pores of the E-face, which becomes more apparent to the observer when such a preparation was compared with an etched specimen (Fig. 5, *A* and *B*). Grazing thin sections, also as observed by others (8, 10), dimly displayed streaks radiating from the central density (Fig. 5*C*).

Lack of ice damage by our freezing technique was confirmed by freeze substitution of diaphragm muscle, kidney, and pancreas, which had been frozen as if for fracture etching on the copper block. Such preparations displayed evenly stained cytoplasm, evidence of the absence of destruction of cellular structure by ice-crystal formation. Pores found in grazing sections of freeze-substituted tissue appeared to be in the same size range as those seen in traditional thin sections. Tissue frozen on a helium-cooled copper block according to the method of Heuser et al. (16), displayed the same fenestral diaphragm structure as that frozen by hand-held hammer on the nitrogen-cooled block.

A similar diaphragmatic structure could be seen in fenestrated capillaries of a variety of tissues: adrenal cortex (Fig. 6*A*), endocrine and exocrine pancreas, as well as kidney. Furthermore, photographic augmentation at $n = 8$ according to the method of Markham et al. (17) revealed identical octagonal symmetry in fenestral diaphragms of all of these tissues (Fig. 6, *B–G*). Most, but not all, fenestral diaphragms could be photographically augmented. Some fenestral diaphragms revealed symmetry of higher multiples of 4, even printed with only eight rotations of 45° (Fig. 6, *C* and *G*).

To label the fenestral diaphragm thus revealed by etching, we injected CF into the circulation. This probe has been shown to bind heavily to fenestral diaphragms but not to plasmalemmal vesicular diaphragms. CF was expected to obscure the "flowers" on luminal surfaces. Untreated specimens of kidney medulla, fractured and etched simultaneously with CF-treated tissue, displayed the now-familiar structure (Fig. 7*A*). Interspersed with the large fenestrae, smaller openings were again apparent. Thin sections disclosed the well-known diaphragms bridging fenestral pores, as well as some "double diaphragms" (Fig. 7*B*). Some capillaries displayed both types of pores: single diaphragms, double diaphragms, as well as plasmalemmal vesicle openings (Fig. 7*C*). The fenestrated capillaries in CF-treated medulla had no fields of flowers, but instead, evenly spaced mounts of particles decorated the luminal surface (Fig. 7*D*). In fracture faces, some of these particles were removed along with membrane half, and the diaphragmatic fibrils were revealed beneath. Smaller pores among the large mounds remained unlabeled. The CF seemed to have higher affinity for the central mesh (Fig. 7*D*, *inset*). The size and shape of the CF particles after etching and platinum replication was identical to that described by Heuser (19) (Fig. 7*D*, *inset*). Thin sections confirmed these results (Fig. 7, *E–F*); CF bound fenestral diaphragms heavily, plasma membrane only patchily, and plasmalemmel vesicular diaphragms rarely, as has been reported by others (13). It penetrated only a very few fenestrae, but was occasionally found inside plasmalemmal vesicles. The double diaphragms did not bind the probe, but neither did they allow its passage (Fig. 7*E*), suggesting that they were not identical to the fenestral diaphragm, and that they were less permeable than the plasmalemmal vesicular diaphragm. Continuous capillaries, also from kidney medulla, had no label on the luminal surface of the plasmalemmal vesicular diaphragm in replicas of etched tissue (Fig. 8*A*), nor was there label on these diaphragms in thin section (Fig. 8*B*). That ferritin had attained these vessels was affirmed by its presence on the plasma membrane surface, readily recognizable in both types of preparations.

Finally, we calculated the average arc length of the widest dimension of the wedge-shaped channels occurring between the radiating fibrils. To do this we used the following formula: [(average pore circumference) − (width of fibril) (average number of fibrils)]/(average number of fibrils) = width of average communicating channel. If the average pore diameter is 600Å, then the average pore circumstance (¶d) equals 188.4 nm. Fibrils measured 7-nm wide, and the mean number was 14, the average number was 15 (Fig. 9). Using these numbers in the above equation, we calculated an average channel width of 5.46 nm. This will be slightly smaller than the actual width in that the platinum shadow augments the width of each fibril by 1–2 nm beyond its actual size (19).

DISCUSSION

In 1969, Clemente and Palade (8) proposed that the communicating channel by which water, solutes, and macromolecules traverse the wall of fenestrated capillaries was at the level of the fenestral diaphragm. Since then, physiologists have done much to elucidate the permeability properties, filtration coefficients, and osmotic reflexion coefficients of primarily continuous capillaries, but unfortunately, not of fenestrated ones (2–4, 20, 21). Morphologic studies, however, have described some of the molecular properties of the fenestral pore itself (1, 8–13). Until now, however, only by chance have grazing sections (8, 10), or photographic augmentation of freeze-fracture replicas (10), revealed faint clues as to the internal structure of the fenestral diaphragm. In this article, replicas portraying great vistas of fenestral diaphragms are displayed, the result of the application of a new technique in tissue preparation. In the ensuing discussion, we will address the following points: (*a*) a summary description of the fenestral diaphragms and plasmalemmal vesicular diaphragms; (*b*) the evidence that these diaphragms are structurally true and not an artifact of the new technique; and (*c*) the functional implications of the structure.

Diaphragm Structure

The fenestral diaphragm in etched replicas had an average diameter of 60 nm, as has been shown to be the approximate size of the fenestral pore in past studies (1). It was made up of 7-nm fibrils that arose from the pore's brim, interwove in the center, and returned to another point along the brim. The central mesh formed by these fibrils measured 10–12 nm in diameter, and thus corresponded in size and location to the central density identifiable in thin sections (8); it was only sometimes surmounted by a central particle. Precedence for such a structure has been reported: grazing thin sections display radiating streaks suggestive of the fibrils (8, 10); and photographic augmentation of both grazing thin sections and traditional fractures displayed two concentric rings, connected by radial spokes with octagonal symmetry (10).

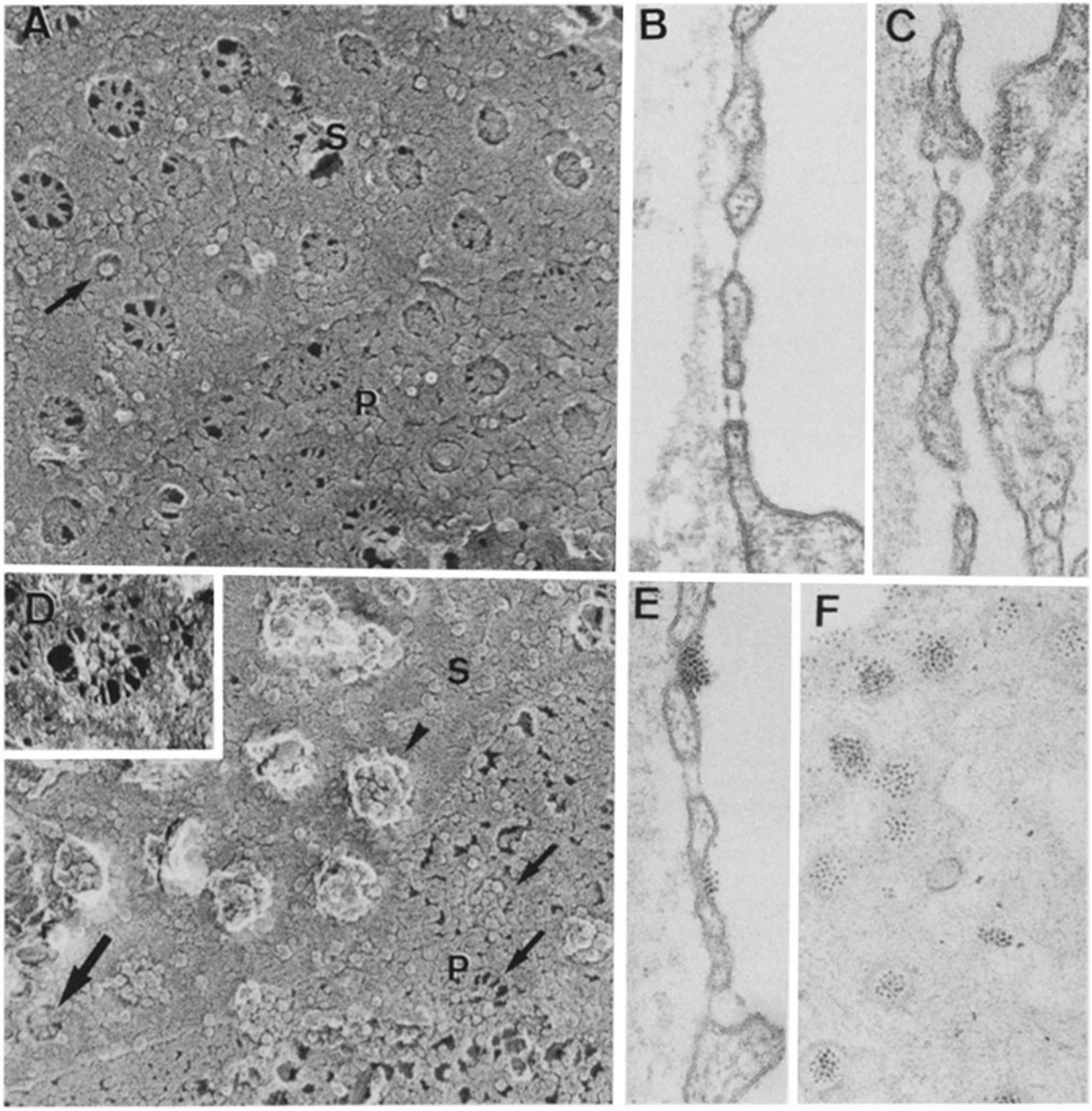

FIGURE 7 (*A*) Untreated peritubular capillaries showing surface (*S*) and P-face (*P*). Fenestral flowers contrast with tiny, PV-like openings (arrow). × 110,000. (*B*) Thin sections of the same tissue also shows single and double diaphragms bridging the fenestral pores. × 90,000. (*C*) All three types of endothelial pores occur in the same peritubular capillary: fenestrae with single or doubled diaphragms, and PV vesicles. × 90,000. (*D*) CF obliterates the fenestral flower (arrowhead) on the luminal surface (*S*), but the tiny, PV-like pore remains undecorated (large arrow). In the P-face (*P*), from which the ferritin has been partially sheared away by the fracturing process, the radiating fibrils can be discerned in rare pores (small arrows). The ferritin particles decorating a single flower are readily identifiable (*inset*). × 110,000 (*inset*, × 150,000). (*E*) Thin sections confirm that ferritin is heaped upon the single fenestral diaphragms and that double diaphragms remain unlabeled. × 90,000. (*F*) Grazing sections demonstrate ferritin concentrated on the diaphragms. × 90,000.

The diaphragms reported here allowed visualization of the geometric shape and dimensions of the communicating channels. These appeared as empty spaces between the fibrils, presumably due to sublimation of water during etching. This channel had the shape of a wedge, and calculations based on average numbers of fibrils and diameter of the pores showed it to have an average maximum arc length of 5.46 nm. This agrees with tracer studies in which fenestral diaphragms are readily permeable to horseradish peroxidase (4.5-nm diam), but not to ferritin (11-nm diam) (1, 8).

The fenestral diaphragms were remarkably different from plasmalemmal vesicular openings. The latter, smaller (40 nm) and less easily etched, had a thick, 10-nm-wide, particulate ridge in P-faces and were not visible in muscle on the abluminal surface. Unlike fenestral diaphragms, those seen on the luminal surface of kidney medulla were consistently decorated

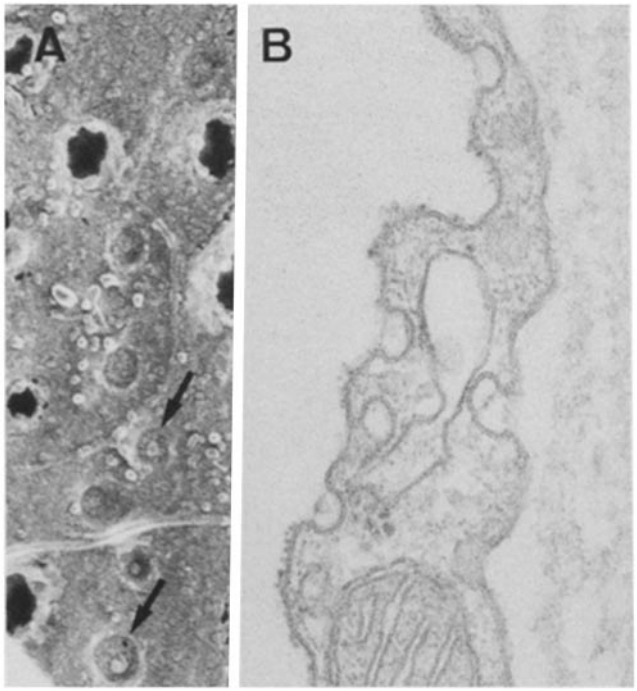

FIGURE 8 (A) Luminal surface of a continuous capillary from kidney medulla. Ferritin balls decorate the membrane surface, but PV openings (arrows) similar to those shown in Fig. 2C, are not labeled. × 107,000. (B) The same tissue in thin section reveals the equivalent results: some ferritin on the luminal surface, but vesicle diaphragms are free of label. × 75,000.

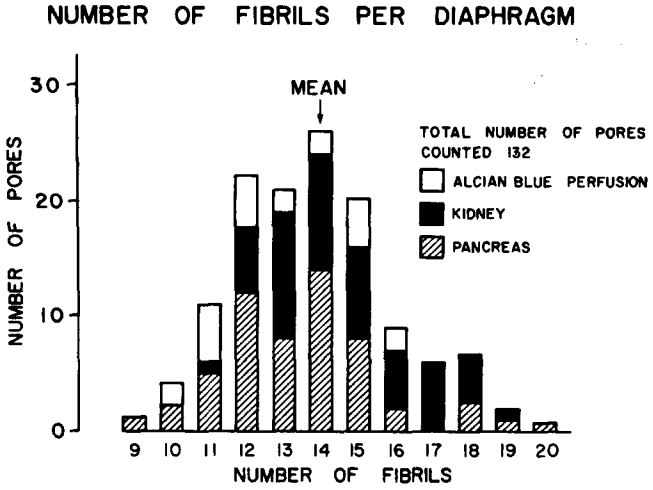

FIGURE 9 Micrographs were selected as for Table I at a magnification of 75,000. Fibrils were counted in all pores in a given micrograph. Fibrils in groups were counted as one unless they could be clearly resolved individually, or they became separate at some point along their length. Broken filaments were counted as one.

with a large central particle. The structure supporting the central particle was not well visualized by this technique, presumably because the distance between the cell membrane and the stomatal particle was too small to allow penetration of a 23° oblique platinum shadow to reach further than 4.4 nm below the surface. As has been reported, they did not bind CF (13). A plasmalemmal vesicularlike opening also frequently occurred among fields of fenestral diaphragms. In this location, however, it was unlikely to be an opening into a vesicle because the endothelial cell body is too thin to accommodate a vesicle. Like the plasmalemmal vesicular opening, and in parallel with the double diaphragm seen in thin sections, these small "pores" among the large fenestral diaphragm did not bind CF. For this reason, we propose them to be the etched correlate of the double diaphragm. The morphologic similarity between the double diaphragms and plasmalemmal vesicular openings supports the contention, originally based upon their lack of CF binding and their similarity in thin sections, that they arise from the same precursor (8). The dissimilarity in these same parameters with fenestral diaphragms argues against the latter also arising from that precursor. Precedence for the morphologic singularity of these two classes of diaphragms is well established: although the fenestral diaphragms bind cationic ferritin, but not lectins, plasmalemmal vesicular diaphragms have the opposite affinity (11–13).

The diaphragmatic structure, so clearly unveiled, seems truly amazing. Could it be produced by an artifact? Since ice can be ruled out because of its absence in freeze-substituted tissue as well as through the fine cytoplasmic texture and lack of holes in membrane in the replicas, we will concentrate on four points which argue the validity of the basic structure:

(*a*) Flowerlike diaphragms did not occur in all membranes or within all membrane pores; they were only apparent in endothelia known to have fenestral diaphragms, such as kidney peritubular capillaries and capillaries in endocrine and exocrine pancreas, and adrenal cortex. Glomerular capillary fenestrae were empty, nor did the fenestral diaphragms appear in continuous capillaries of muscle. They did reside side by side with plasmalemmal vesicular openings in mixed capillaries of the exocrine pancreas, demonstrating that the differences in these two types of endothelial membrane specializations were not elicited by inadvertent differences in preparation of different tissue. (*b*) The radiating fibrils and octagonality have been reported before (8, 10) as mentioned above. Thus, this configuration should not be a surprise. The consistent diameter of the pore itself also argues for the lack of ice-crystal disturbances, and for the preservation of the internal structure. (*c*) Whereas distribution and location identified the diaphragms as being within the fenestral pore, CF binding confirmed this by obscuring the diaphragmatic flower on luminal surfaces, while leaving plasmalemmal vesicular openings bare. The ends of the fibrils inserting in the pore's brim could sometimes be recognized under the heap of ferritin particles, testifying to the continued existence of the original diaphragmatic structure. (*d*) The calculated arc width of the wedge-shaped communicating channels, 5.45 nm, correlates with tracer studies that predicted the size to be between that of horseradish peroxidase (4.5 nm) and ferritin (11 nm). Unexpectedly, for all their apparent differences, the calculated arc width of the fenestral diaphragms also correlates perfectly with the width of a slit-shaped channel predicted for continuous capillaries, 5.1–5.76 nm (20, 21). It could be that it is only the addition of the anionically charged heparin-derivative that contributes to the difference between these two diaphragms, and that basic structural components are the same. Furthermore, despite their basis on continuous capillaries, the suggestion by physiologists of a separate channel for water may be borne out by fenestral capillary diaphragms because they have a second, tiny quadrangular channel occurring in the central mesh (20, 21).

Although these arguments support our contention that the flowerlike structure is a true representation of the fenestral diaphragm in the living animal, the following reservations need to be considered: first, processing steps may alter these delicate structures. Perfusion pressure, lack of protein in fixative solutions, and length of time of fixation could all influence the structure. In addition, movement of water may occur during the freezing step if one area of tissue freezes more rapidly than another, thus changing the osmotic environment and causing dehydration in the more slow-to-freeze regions. Finally, any delicate substance could be lost from the interstices of the fibrils during etching or replica cleaning. Because octagonal symmetry suggests numbers of fibrils in multiples of eight, but the calculated average diaphragm had only 15 fibrils rather than 16, it is likely that an average of one fibril per diaphragm is artifactually lost during processing.

These reservations render suspect the heterogeneity of the diaphragm in a given field. Because so many show marked photographic augmentation at $n = 8$, such heterogeneity would seem to be a result of tissue processing. On the other hand, this disparity could also be interpreted as a real phenomenon reflecting the dynamics of the diaphragm. Perhaps it opens and closes like the aperture of a camera. Previous evidence for this includes observations that horseradish peroxidase and other small tracer molecules do not traverse all diaphragms at the same rate (21, 22), and the larger, native ferritin penetrates a few, but not all diaphragms (8, 23). Physiologic studies also contribute indirect evidence for dynamic responses of capillary endothelium, in that permeability characteristics of continuous capillaries change rapidly depending on the protein content of the perfusate (21, 24), even when uncharged proteins, i.e., unlikely to stick to the diaphragm, are used. That the fenestral diaphragm may also respond to the ionic strength of its environment, even after glutaraldehyde fixation, was demonstrated here by its size and shape change when treated with distilled water. That alcian blue prohibited, to a large extent, the effect of low tonicity challenges us to hypothesize that binding to the anionic diaphragm by a cationic dye in some way stabilizes it more than glutaraldehyde fixation alone. Clearly, there is room for both artifact and heterogeneity in the size of the communicating channels, as created by distribution of radial fibrils.

The question of whether or not the fenestral diaphragm responds dynamically to its milieu, and many others regarding capillary permeability, can be readily answered now that the fenestral diaphragm can be so clearly visualized.

The authors thank Dr. Dan Friend for his constant support and inspiration, Mr. Georges Aligazakis for technical help, and Nadine Dupont for untiring secretarial assistance. We give special thanks to Dr. Dennis Brown for his advise in perfusion techniques for optimal preservation of kidney ultrastructure.

This study was supported by the Swiss National Scientific Foundation, Grant No. 3.460.83.

Received for publication 18 May 1984, and in revised form 9 September 1984.

REFERENCES

1. Simionescu, N. 1983. Cellular aspects of transcapillary exchange. *Physiol. Rev.* 63:1536–1577.
2. Crone, C., and O. Christensen. 1978. Transcapillary transport of small solutes and water. *Int. Rev. Physiol.* 18:149–213.
3. Renkin, E. M. 1979. Relation of capillary morphology to transport of fluid and large molecules: a review. *Acta Physiol. Scand. Suppl.* 463:81–91.
4. Bundgaard, M. 1980. Transport pathways in capillaries in search of pores. *Annu. Rev. Physiol.* 42:325–336.
5. Pappenheimer, J. R. 1953. Passage of molecules through capillary walls. *Physiol. Rev.* 33:387–423.
6. Palade, G. E., M. Simionescu, and N. Simionescu. 1979. Structural aspects of the permeability of the microvascular endothelium. *Acta Physiol. Scand. Suppl.* 463:11–32.
7. Rhodin, J. A. G. 1962. The diaphragm of capillary endothelial fenestrations. *J. Ultrastruct. Res.* 6:171–185.
8. Clementi, F., and G. E. Palade. 1969. Intestinal capillaries. I. Permeability to peroxidase and ferritin. *J. Cell Biol.* 41:33–58.
9. Hurley, J. V., and N. McCallum. 1974. The degree and functional significance of the escape of marker particles from small blood vessels with fenestrated endothelium. *J. Pathol.* 113:183–196.
10. Maul, G. G. 1971. Structure and formation of pores in fenestrated capillaries. *J. Ultrastruct. Res.* 36:768–782.
11. Simionescu, M., N. Simionescu, J. E. Silbert, and G. E. Palade. 1981. Differentiated microdomains on the luminal surface of the capillary endothelium. II.. Partial characterization of their anionic sites. *J. Cell Biol.* 90:614–621.
12. Simionescu, M., N. Simionescu, and G. E. Palade. 1982. Differentiated microdomains on the luminal surface of capillary endothelium: distribution of lectin receptors. *J. Cell Biol.* 94:406–411.
13. Simionescu, M., N. Simionescu, and G. E. Palade. 1981. Differentiated microdomains on the luminal surface of the capillary endothelium. I. Preferential distribution of anionic sites. *J. Cell Biol.* 90:605–613.
14. Kanwar, Y. S., and M. G. Farquhar. 1979. Anionic sites in the glomerular basement membrane: in vivo and in vitro localization to the laminae rarae by cationic probes. *J. Cell Biol.* 81:137–153.
15. Krakower, C. A., and S. A. Greenspan. 1951. Localization of the nephrotoxic antigen within the isolated renal glomerulus. *Arch. Pathol.* 51:629–639.
16. Heuser, J. E., T. S. Reese, and D. M. Landis. 1972. Preservation of synpatic structures by rapid freezing. *Cold Spring Harbor Symp. Quant. Biol.* 40:17–24.
17. Markham, R., S. Frey, and G. J. Hills. 1963. Methods for the enhancement of image detail and accentuation of structure in electron microscopy. *Virology.* 20:88–102.
18. Behnke, O., and T. Zelander. 1970. Preservation of intercellular substances by the cationic dye alcian blue in preparative procedures for electron microscopy. *J. Ultrastruct. Res.* 31:424–429.
19. Heuser, J. E. 1983. Procedure for freeze-drying molecules adsorbed to mica flake. *J. Mol. Biol.* 169:155–195.
20. Michel, C. C. 1979. Filtration coefficients and osmotic reflexion coefficients of the walls of single frog mesenteric capillaries. *J. Physiol. (Lond.).* 309:341–355.
21. Michel, C. C. 1979. The investigation of capillary permeability in single vessels. *Acta Physiol. Scand. Suppl.* 463:67–74.
22. Simionescu, N., M. Simionescu, and G. E. Palade. 1972. Permeability of intestinal capillaries: pathway followed by dextrans and glycogens. *J. Cell Biol.* 53:365–392.
23. Loudon, M. F., C. C. Michel, and I. F. White. 1979. The labeling of vesicles in frog endothelial cells with ferritin. *J. Physiol. (Lond.).* 296:97–112.
24. Levick, J. R., and C. C. Michel. 1973. The effect of bovine serum albumin on the permeability of frog mesenteric capillaries. *Q. J. Exp. Physiol.* 58:87–97.